NASCAP-2K AS A PIC CODE

M. J. Mandell
Science Applications International Corporation
10260 Campus Point Dr., M.S. A1,
San Diego, CA, 92121
Phone: 858-826-1622
Fax: 858-826-1652
E-mail: myron.j.mandell@saic.com

D. L. Cooke
Air Force Research Laboratory/VSBS

Abstract

Nascap-2k can be used to calculate plasmadynamic effects as well as steady-state charging and current collection. In this paper we consider electron dynamics in the sheath of a VLF antenna. We estimate the sheath size, and show 1-D calculations for both sine wave and square wave excitation. The results show strong electrostatic plasma oscillations at the sheath edge. Then we use Nascap-2k to duplicate the square wave results through the first maximum in the plasma oscillation, obtaining excellent agreement with the 1-D results. This opens the door to fully 3-D dynamic VLF antenna calculations.

Introduction

There is current interest in generating VLF waves in space for the purpose of controlling the trapped electron population (Inan *et al*., 2003). A transmitting antenna for this purpose would be several inches in diameter, tens of meters long and have bias amplitudes of hundreds of volts. It would interact with a large volume of the surrounding plasma, and be a major driver for spacecraft potential. Thus, it is of major interest to be able to simulate dynamically and in 3-D the antenna together with its host spacecraft and the surrounding plasma.

Nascap-2k, through its DynaPAC heritage, contains the features needed to do this type of problem. However, these features have not been fully exercised since the days of SPEAR II (Cohen, 1995). In studying the CHAWS experiment (Davis, *et al.*, 1999), ion trajectories were used to calculate steady-state, self-consistent charge densities and space potentials, and we have exercised the ability to do PIC ions with barometric electron densities. For the antenna problem we would like to do both electrons and ions using PIC. (Note, however, that Nascap-2k only solves Poisson's equation, rather than the full Maxwell equations, so it computes only curl-free, quasi-static fields.)

In this paper we describe the antenna problem, and, for baseline parameters, show the solution, as calculated by a 1-D PIC code, for electron dynamics in the sheath. We then pose a nearly identical problem for solution with Nascap-2k, demonstrate that the solutions agree, and show the graphics. We were nearly able to do the problem using the current release of Nascap-

2k, editing scripts within the GUI and some of the generated ASCII input files. In the end, one line of code had to be changed to obtain a correct result.

Statement of Problem

The objective is to simulate the dynamic sheath around a negative thin rod. We avoid positive polarity because the positive half of the antenna will collect copious electrons, so the maximum potential it can reach is determined by numerous unknown factors, such as the relative size of the spacecraft and antenna. We wish to do this with realistic values of plasma density, ion mass, applied voltage, frequency, magnetic field, and spacecraft velocity. The arbitrary directions of the latter two require a 3-D code. A 1-D (radial) code can handle magnetic field either parallel to the antenna or circumferential (as would be caused by current flowing in the antenna).

Sheath Size Estimate

The sheath (defined as the region from which electrons are excluded) can be quite large, even for a fairly modest potential of about 100 volts. To calculate the sheath size, we specify the electric field at the antenna radius, R_0. We assume that the external space between the antenna and the sheath is filled with ions at ambient density, ρ. The electric field at any radius, r, between the antenna and the sheath is

$$E(r) = \frac{\rho e(r^2 - R_0^2)}{2\varepsilon_0 r} - \frac{a}{r}E(R_0)$$

The sheath condition is $E(R_s)=0$, where R_s is the sheath radius. We then integrate the electric field from R_s to R_0 to determine the corresponding potential.

Figure 1 shows the relation between applied potential and sheath radius for a 10 cm diameter antenna. At a density of 10^{12} m^{-3} the sheath radius at 100 volt bias is about 15 cm, and grows to nearly a meter at a density of 10^{10} m^{-3}. The calculations to follow assume a density of 3×10^{11} m^{-3}, giving a sheath radius of about 20 cm.

Baseline Parameters

Table 1 shows the baseline parameters for the calculation. Density of 3×10^{11} m^{-3} is chosen so that the sheath is large compared with the wire but still very tractable computationally. In general the plasma is cold, but 0.1 eV is used in those places where temperature is required. The antenna frequency is set to 100 kHz, and the process is followed for a half-period of 5 microseconds. To see the effect of magnetic field, a field of 0.5 gauss is chosen. The ordering of the plasma frequency, electron gyrofrequency, and applied frequency is $\omega_p > \omega_c > 2\pi f$.

Table 1. Parameters for baseline calculations.

Plasma Density	3×10^{11} m^{-3}
Electron Temperature	0.0 or 0.1 eV
Plasma Frequency	3.1×10^{7} s^{-1}
Antenna Frequency	100 kHz
Magnetic Field	0.0 or 0.5 gauss
Electron Gyrofrequency	0.0 or 8.8×10^{6} s^{-1}
Ion Species	O^{+}

1-D Calculations

A simple one-dimensional finite element code was written to simulate quasistatic plasma-dynamics about a long cylindrical antenna. The computational domain extended out to one meter from an antenna radius of 5 cm, and was divided into 1000 zones in equal increments of r^2. Two ion macroparticles and two electron macroparticles were placed in each zone, with each macroparticle having equal charge. The simulation was run for 2000 timesteps of 2.5 nanoseconds each, making up the 5 microsecond half-period for the 100 kHz frequency. When electrons left the computational space they were replaced by thermal electrons.

Figure 2 shows the potential profile at various times in the calculation. As expected, the potential is rapidly screened to about the expected sheath radius as electrons are expelled from the sheath. At certain times a positive potential region appears. This is an effect of electron inertia, as the moving electrons do not stop of their own accord, but must be attracted back towards the sheath boundary. In Figures 3-6 we plot (1) the maximum potential at times when a positive region appears; (2) the location of the maximum potential; and (3) the location of the sheath edge, indicated by a sharp drop in the charge density from nearly the ambient ion density to nearly zero.

Figures 3 and 4 show results for a half sine wave, for which the applied negative potential continuously rises and returns to zero. The magnitude of the potential maximum is 8-10 volts, and the oscillation frequency is somewhat less than the electron plasma frequency. The sheath edge occurs at a radius of about 20 cm as calculated above, with oscillations of about two cm. The potential maximum, when it occurs, is just inside the sheath edge.

Two differences can be noted between the unmagnetized (Figure 3) and magnetized cases. First, in the unmagnetized case the potential goes completely non-positive between peaks, whereas in the magnetized case a positive peak forms inside the outer boundary. This occurs because the magnetic field inhibits inward diffusion of the thermal electrons. Second, in the unmagnetized case the sheath remains at the end of the pulse, even though the potential goes to zero, while in the magnetized case the sheath disappears. This occurs because the magnetic field traps inbound electrons in the sheath region, whereas in the absence of magnetic field inbound electrons collide with the antenna.

Square wave calculations were done in 1-D to compare with the Nascap-2k calculations below, and are shown in Figures 5 and 6. Much stronger plasma oscillations are seen, with the

initial oscillation at 75 volts. The sheath edge oscillates 10 cm on either side of its average position at 20 cm, and the peak potential occurs well inside the sheath. Application of the 0.5 gauss magnetic field doubles the rate of decay of the oscillations.

3-D Calculations

Three-dimensional calculations were done with Nascap-2k to demonstrate the feasibility of such calculations. Figure 7 shows the Nascap-2k antenna model embedded in a nested grid. The antenna consists of two square rods, each 10 cm on a side and 4 m long. The outer boundary of the grid is a square 1.32 m on a side. The coarse resolution is 11 cm, with 5.5 cm resolution near most of the antenna, and 2.75 cm resolution in a limited region. Initially, 8 electron macroparticles and 8 ion macroparticles were placed in each zone, positioned so as to represent a uniform charge distribution in the context of the nonlinear interpolants. A negative 100 volt square wave was applied to half of the antenna, and each timestep consisted of (1) tracking the particles for 2.5 nanoseconds, (2) sharing the particle charge to the nodal coefficients in accordance with the nonlinear interpolants, and (3) recalculating the potential in preparation for the next tracking phase.

The initial state is represented in a 3-D view in Figure 8, and a planar view in Figure 9. Each of Figures 9-12 shows a plane of potentials with a plane of electron macroparticles just above it, positioned as shown in Figure 8. (Ion macroparticles have the same initial configuration, but move negligibly during the simulation time.) Note that the apparent high density of particles in the subdivided region is balanced by correspondingly reduced particle weight. Comparing Figure 10 with Figure 9, we see that the potentials change little in the first 25 nanoseconds, but they change considerably in the next 25. Figure 11 shows the electron motion, leading to sheath radii of 9 cm at 25 nanoseconds and 18 cm at 50 nanoseconds. Figure 11 shows the effects of the square cross-section. Particles that started out near the flat, low-field region have moved considerably less than those that started out near the high-field corners.

The simulation was run up to the first potential maximum, which occurred at 137.5 nano-seconds. Figure 12 shows that, at this time, there is a high, broad maximum in the potential, with electrons excluded from a region that extends well beyond the location of the potential maximum. Figure 13 shows another view of the final configuration, with potentials in a plane containing the antenna. Note that there is no apparent difference between the potentials in the highly resolved region and in the less resolved region, suggesting that the highest level of resolution may not be needed.

Figure 14 shows the development of the sheath radius and maximum potential calculated by Nascap-2k, compared with the 1-D sheath radius result. The maximum potential of 75 volts, as well as the time of first maximum (140 ns) is in excellent agreement with the one dimensional result. The maximum sheath radius calculated by Nascap-2k is larger than the 1-D result in proportion to the effective larger size of the 10 cm square antenna vs. the 10 cm diameter round antenna.

Conclusions

Electron dynamics are important in the very large sheaths of VLF antennas under space conditions. Large electrostatic oscillations are to be expected, producing at times positive potential regions about a negative antenna. The amplitude of the oscillations is waveform dependent.

Nascap-2k is shown to have the ability to perform quasi-electrostatic PIC simulations of sheath dynamics in fully 3-D geometry. This is important because such simulations can take into account the presence of the host spacecraft and arbitrary directions of magnetic field and spacecraft velocity.

To do the calculations shown here, scripts needed to be edited within the GUI, and ASCII input files needed to be edited. Only one line of source code had to be changed to obtain a correct result. Thus, an advanced user could do such calculations with the current Nascap-2k release, provided he was given access to the one altered DLL. Future Nascap-2k development will include tuning to make quasi-electrostatic PIC calculations more accessible to less advanced users, as well as features needed for more lengthy calculations, such as introducing thermal electrons at boundaries.

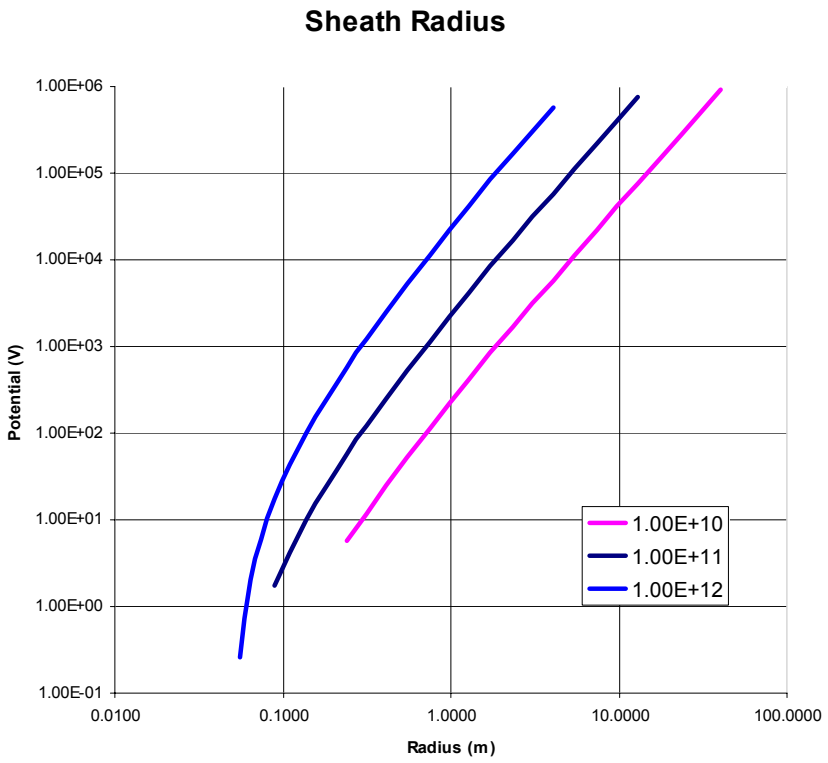

Figure 1. Potential vs. sheath radius for negative applied potential on a 10 cm diameter antenna. Curves for three different plasma densities are shown.

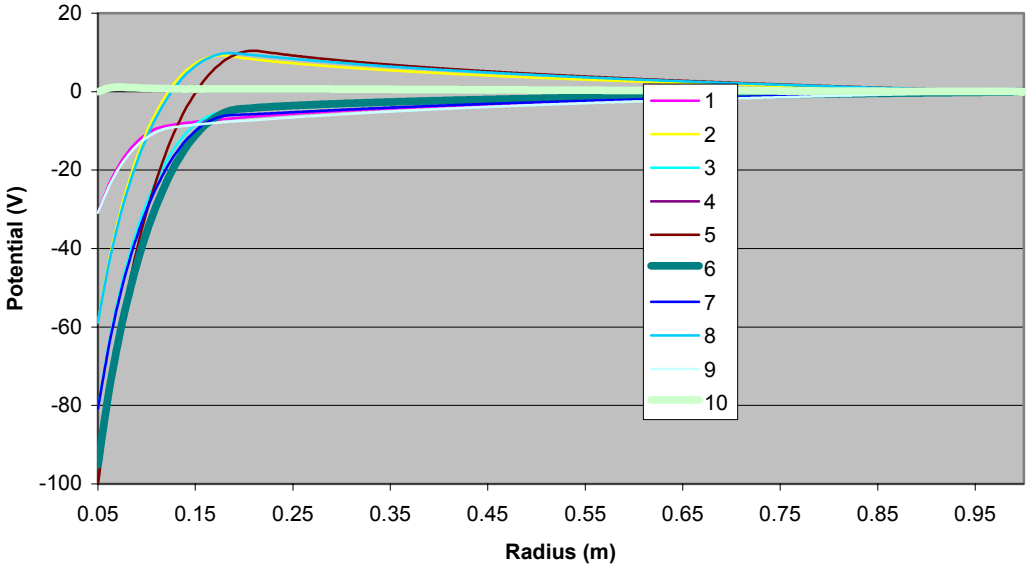

Figure 2. Potential profile at various times during the 1-d calculation.

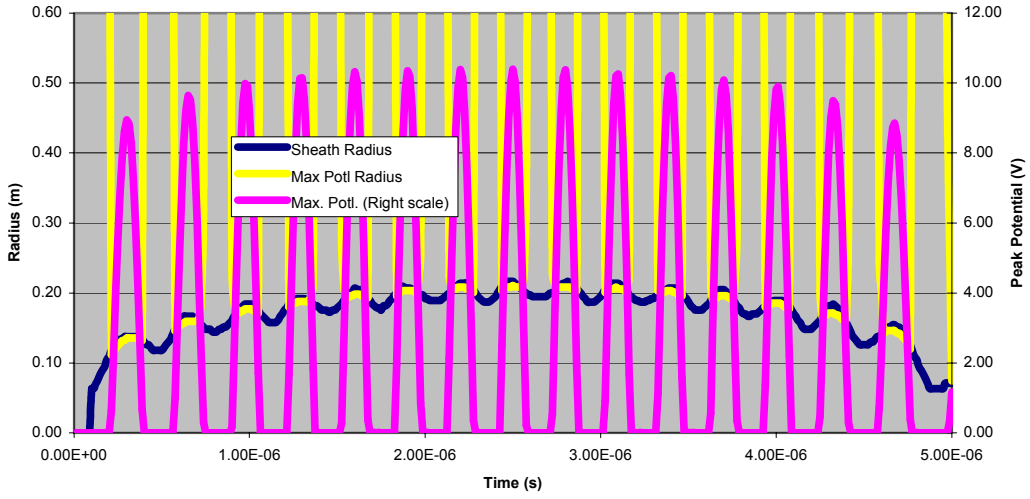

Figure 3. Simulation results for half sine wave and no magnetic field, showing peak positive potential (magenta curve, right scale), location of peak (yellow curve, left scale) and location of sheath edge (dark curve, left scale).

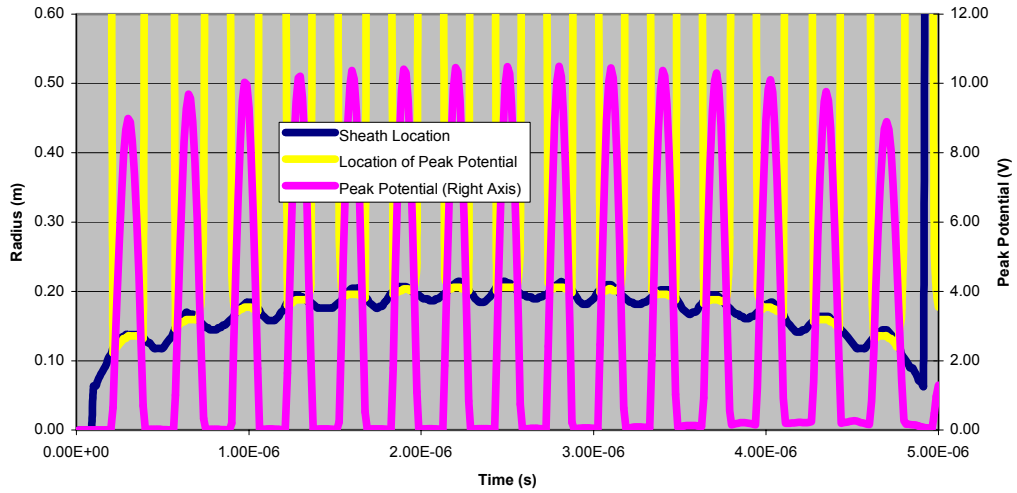

Figure 4. Same as Figure 3, for half sine wave with magnetic field of 0.5 gauss.

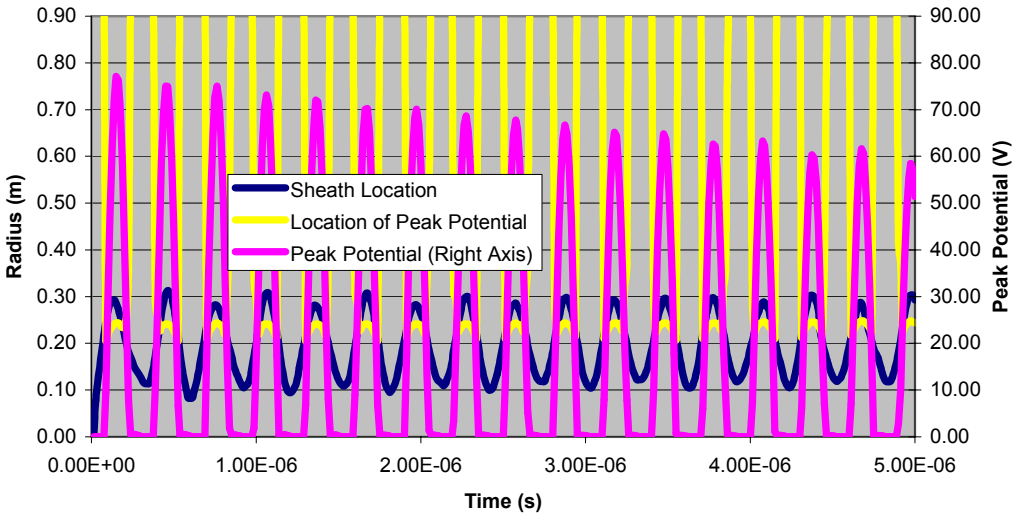

Figure 5. Same as Figure 3, for square wave and zero magnetic field.

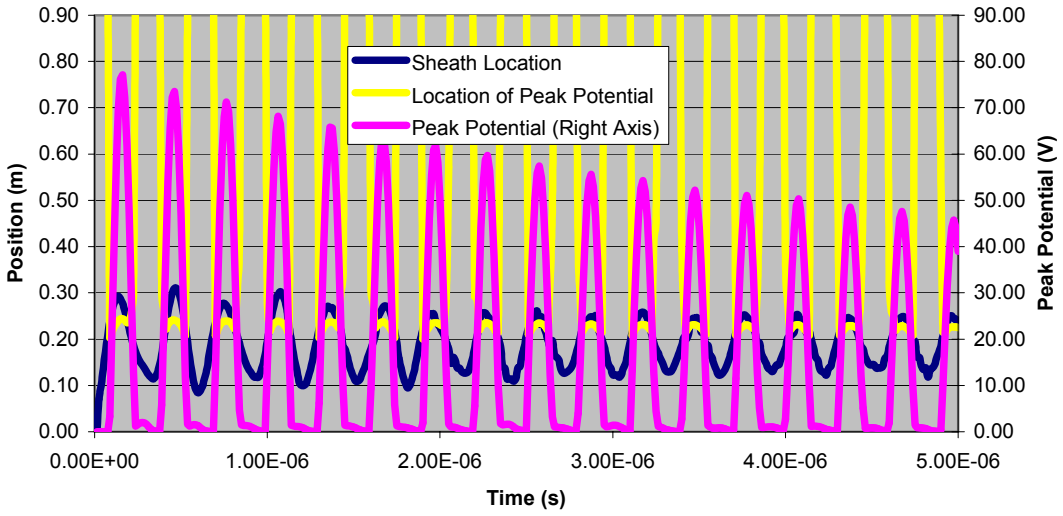

Figure 6. Same as Figure 3, for square wave with 0.5 gauss magnetic field.

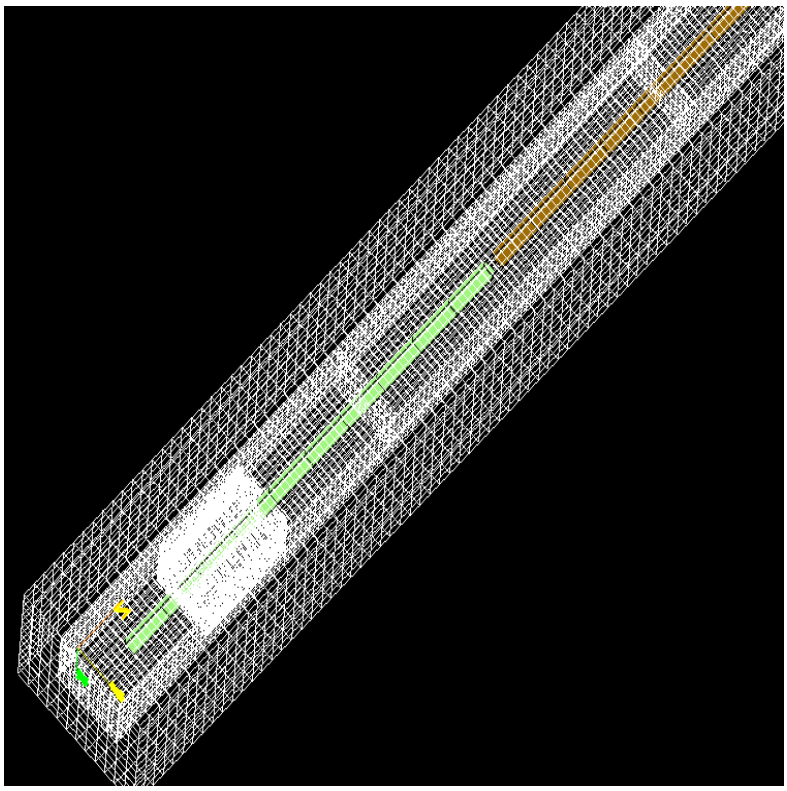

Figure 7. Nascap-2k antenna model, showing antenna and gridding.

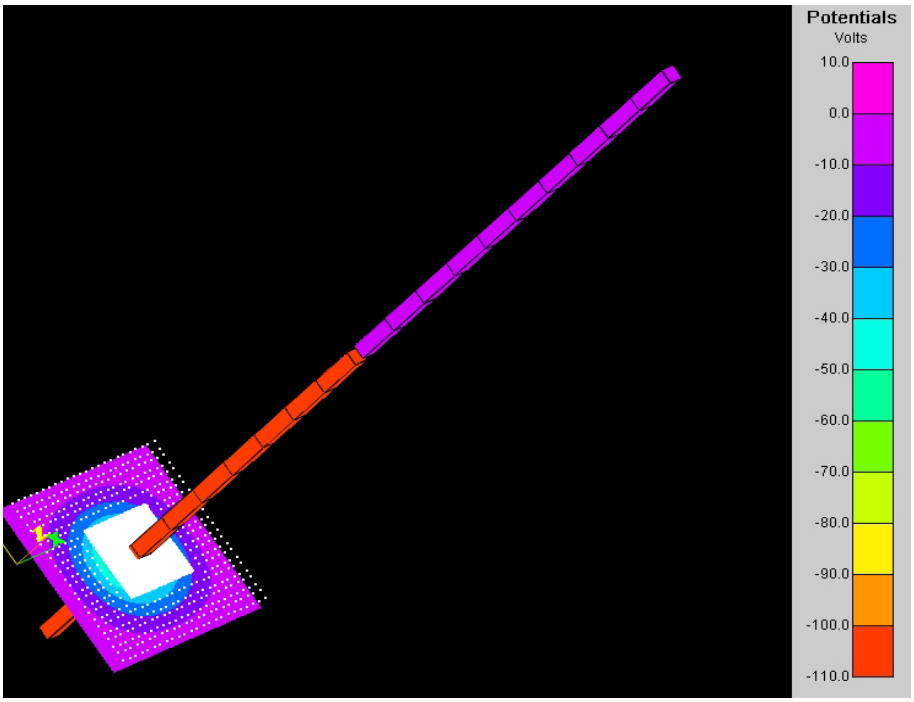

Figure 8. Nascap-2k antenna model showing potentials and particle positions after 2.5 nanoseconds.

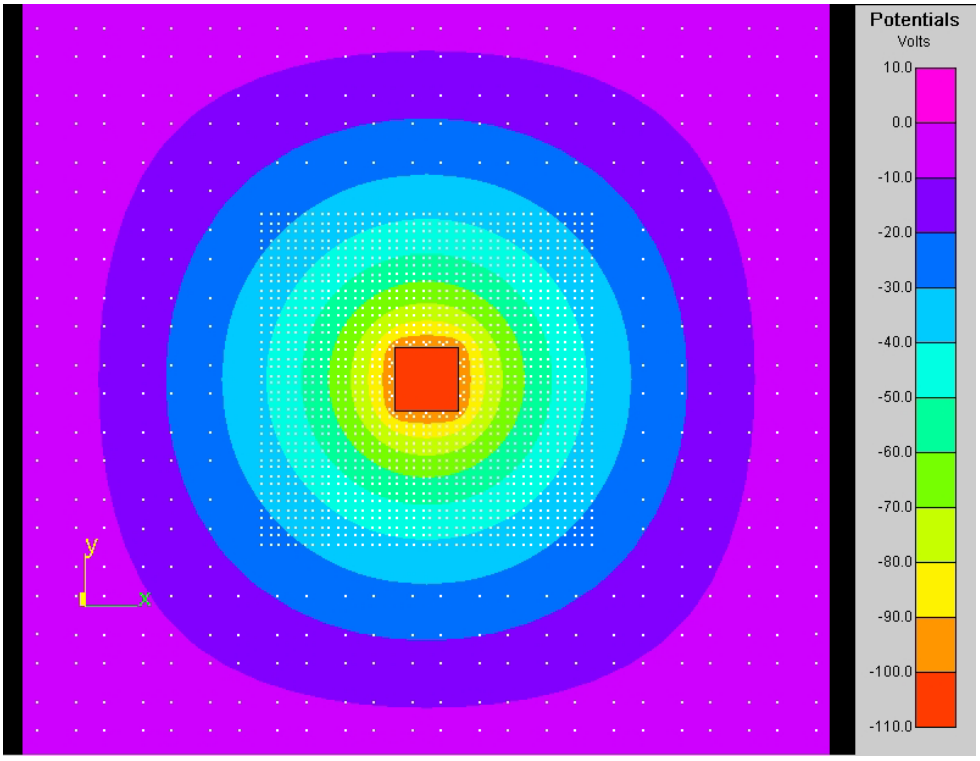

Figure 9. Planar view of initial potentials and particles, as shown in Figure 8.

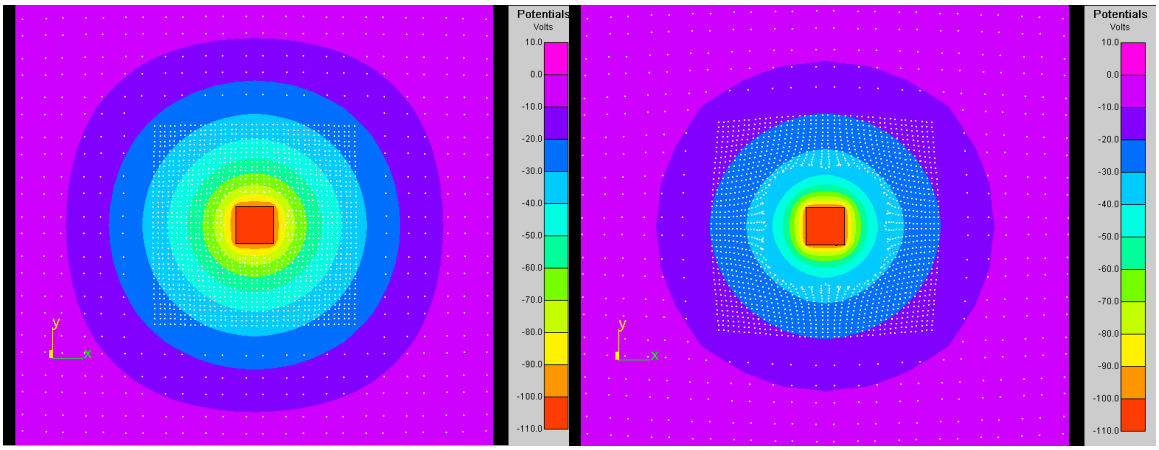

Figure 10. Particles and potentials after 25 nanoseconds (left) and 50 nanoseconds (right).

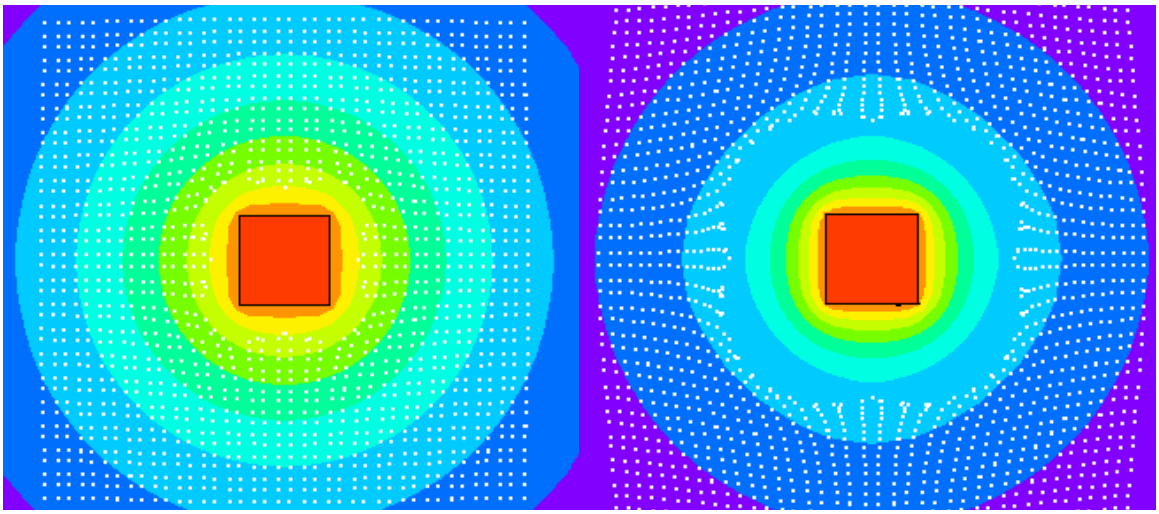

Figure 11. Blowup of Figure 10, showing a sheath radius of 9 cm after 25 nanoseconds (left), and about 18 cm after 50 nanoseconds (right).

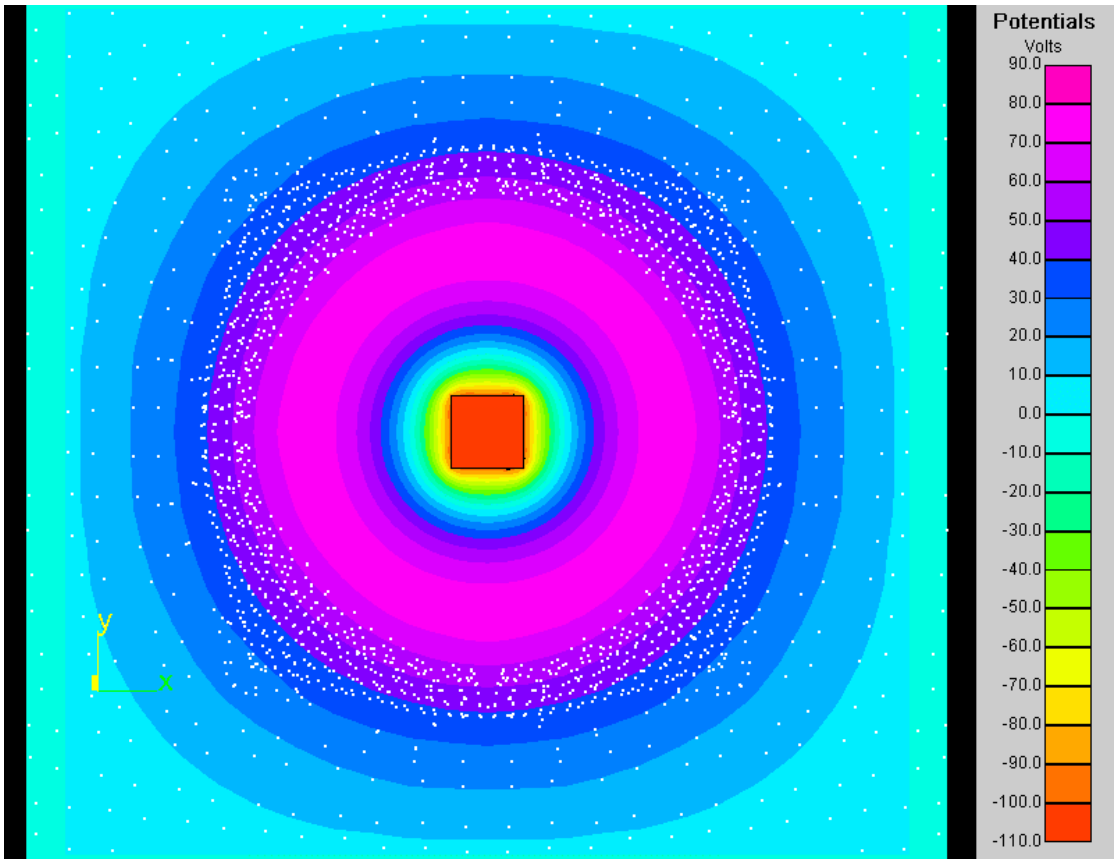

Figure 12. Potentials and particles at time of maximum positive potential.

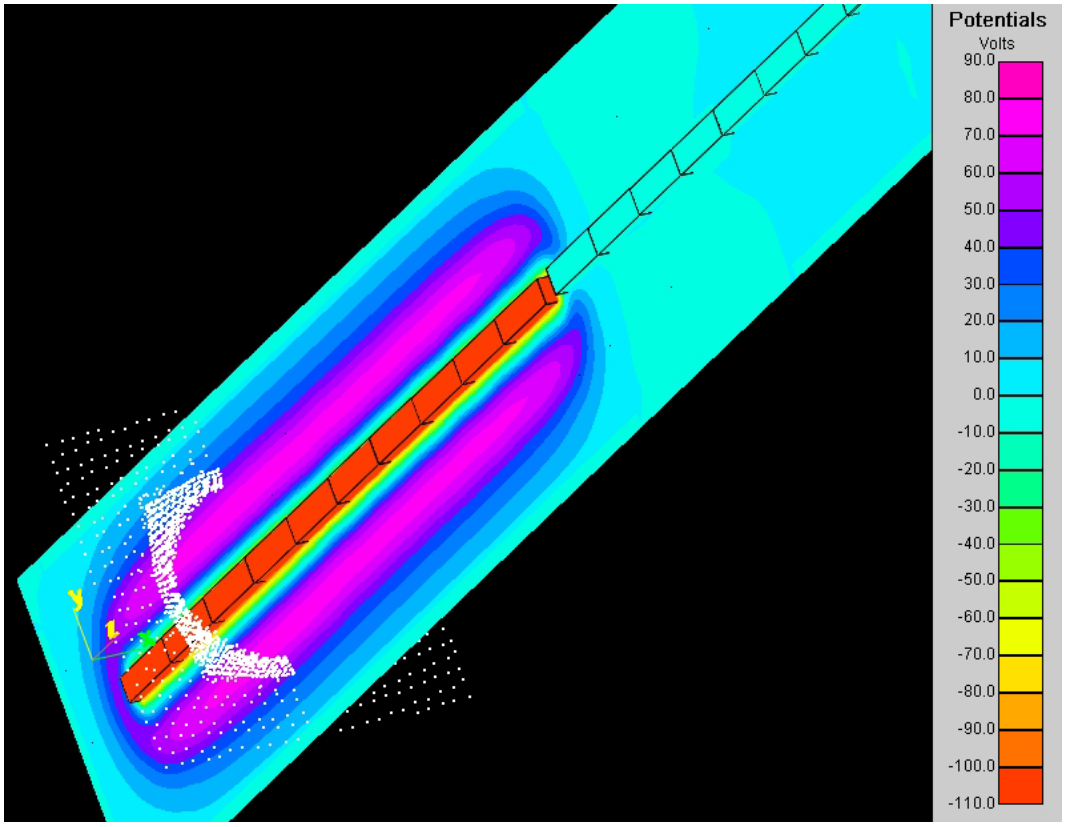

Figure 13. Another view of the final configuration (at 137.5 ns), showing potentials in a plane containing the antenna.

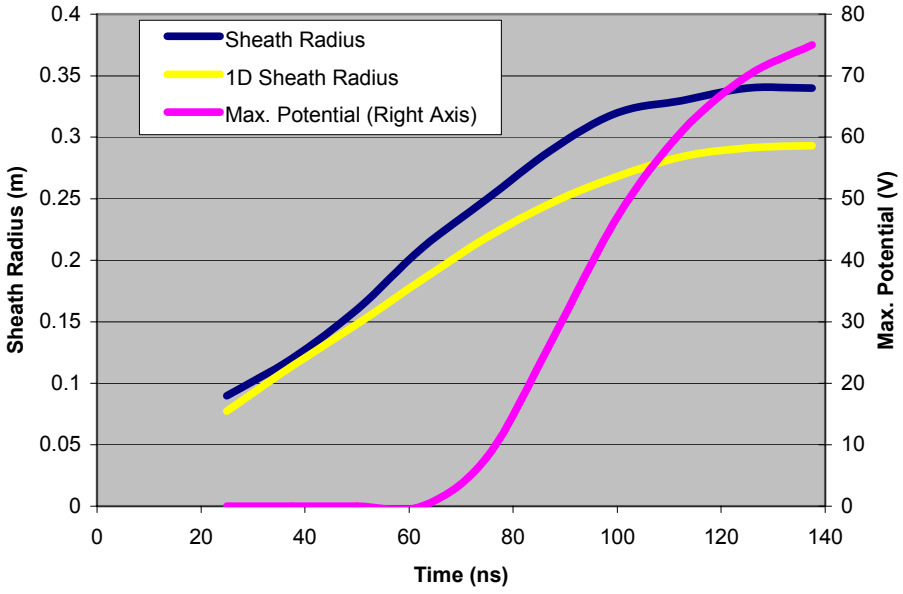

Figure 14. Nascap-2k results for sheath radius (dark curve) and maximum potential (magenta curve, right scale) compared with 1-D sheath radius results (yellow curve).

References

1. Cohen, H. A., F. M. Lehr and T. G. Engel (eds.), Spear II – High Power Space Insulation, Lubbock: Texas Tech University Press, 1995.

2. Davis, V.A., M.J. Mandell, D.L. Cooke and C.L. Enloe, "High-voltage interactions in plasma wakes: Simulation and flight measurements from the Charge Hazards and Wake Studies (CHAWS) experiment," Journal of Geophysical Research 104, No. A6, 12,445-12459, June 1999.

3. Inan, U. S., T.F. Bell, J. Bortnik and J.M. Albert, "Controlled precipitation of radiation belt electrons", Journal of Geophysical Research 108, No. A5, SMP 6-1, May 2003.